IJEMD-BMCR, (3) 2 (2025) https://doi.org/ 10.54938/ijemdbmcr.2025.03.1.477

International Journal of Emerging Multidisciplinaries:
Biomedical and Clinical Research

Research Paper
Journal Homepage: www.ojs.ijemd.com
ISSN (print): 2957-8620 ISSN (online): 2960-0731

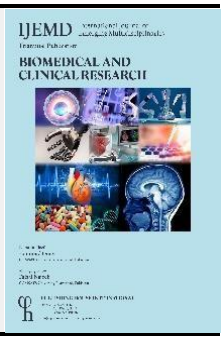

Reynolds Number-dependent Flow Dynamics of Twin Non-Circular Particles in a Vertical Channel : Twin Non-circular Particles Interaction

Muhammad Shahid [1*], Iqra Khalil [2], Muhammad Izhar Ul Haq [2]

1. Department of Mathematics, Air University, PAF Complex, Islamabad 44000, Pakistan
2. Department of Mathematics, Government Boys Postgraduate College Abbaspur, Poonch 12200, AJK, Pakistan

Abstract

A numerical study of falling particles in the fluid domain has been presented in Reynolds number perspective. An analysis for the movement of non-circular particles i.e. triangle, square and pentagon has been conducted. The simulations are carried out for four different Reynolds numbers which are 100, 200, 300 and 1000. The numerical results are found for x- and y-components of velocity profile and trajectory paths of twin particles settling in the channel. At each Reynolds number the results have been compared with particle's shape. Furthermore, the data in tabular form has been presented for minimum x-and y-velocity indicating time for velocity of falling particle in the computational domain, also mentioned the height. The minimum distance between twin particles indicating time at which the minimum distance has been achieved and the height it attains at that time. The simulations are conducted by using fictitious boundary method (FBM) combined with an Eulerian approach, which has been utilized for expressing the free movement of particles in the channel. We applied an explicit volume integral approach for finding the hydrodynamic forces exerted on the surfaces of particle. The numerical simulations are carried out using a multigrid finite element solver FEATFLOW in the fluid flow.

Keywords: Particulate Flow, Fictitious Boundary Method (FBM), General Shaped Particles, Multigrid, Reynolds Number.

1. INTRODUCTION

Particulate flows have a wide range of applications in different fields such as, industrial, environmental, medical and geophysics. In industrial sector these flows are used in fluidized beds, coal combustion in

Email Addresses : mshahidch@outlook.com (M. Shahid *), iqrakhalil301969@gmail.com (I. Khalil) , muhammad.izhar0011@gmail.com (M. I. Haq)

boilers, lubricated transport, paper pulp manufacturing, slurry handling and fuel injection systems. In medical fields particulate flows have applications such as blood flow with suspended cells, nano-particle transport in the body, food manufacturing and seed coating and treatment. Moreover, particulate flow plays a crucial role in areas of environment and geophysics such as filtration, melting, the purification of petroleum-based fluids and solidification. In natural processes these flows also frequently occur in sedimentation processes, transport in rivers and streams, dust storms, volcanic ash and pyroclastic flows and hydrothermal vent particulate plumes. In numerous cases, these flows involve particles suspended in fluids restricted within complex, time-dependent boundaries. From numerical point of view, it is very difficult to analyze the motion of these particles due to continuous remeshing of computational grid.

[23] investigated the results of the dynamics of suspended particles by utilizing the fictitious boundary method with a multigrid finite element solver (FEATFLOW) to simulate particle-fluid interactions. They considered five distinct shapes which are triangle, ellipse, rectangle, square, and star interacting within a fluid channel. The authors analyzed key hydrodynamic properties such as drag/lift and terminal velocity for both single and twin particles under various initial orientations. They diagnosed complex behaviors like drafting, kissing and tumbling phenomenon. Moreover, their results exhibited that particle shape significantly affects settling behavior in the fluid channel. [1] proposed a coupled two-dimensional model using the Discrete Element Method (DEM) and the Lattice Boltzmann Method (LBM) to simulate fluid flow in porous media. An implicit Immersed Boundary Method (IBM) was used to accurately capture fluid-solid interactions without requiring user-defined penalty parameters. The model confirmed strong agreement with theoretical results, proving its effectiveness in simulating complex pore-scale flow phenomena.

[2] conducted a numerical investigation of solid particle motion and interaction in a fluid-filled channel using the Fictitious Boundary Method (FBM) within an Eulerian framework. The study analyzes particle-particle and particle-fluid interactions, including phenomena like drafting, kissing and tumbling, using a collision model based on Glowinski and others. Results show how particle size, initial position, and mesh refinement affect sedimentation dynamics and hydrodynamic behavior during interactions. Shahid *et al.* discussed the computational investigation on drag forces experienced by bluff bodies due to non-circular particles (ellipse, square, and pentagon) settling in a vertical fluid channel. They used the fictitious boundary method with a multigrid finite element solver (FEATFLOW) to simulate particle–fluid interactions, incorporating a modified repulsive force collision model. Their analysis expressed trajectory behavior and drag coefficients under various obstacle arrangements and gap sizes to understand complex particle–obstacle dynamics.

[4] numerically investigated the sedimentation dynamics of a two-dimensional elliptical particle in a Newtonian fluid using both lattice Boltzmann and finite-element methods. They analyzed on how flow patterns are influenced by boundary effects, density ratio, aspect ratio and channel blockage ratio. They identified five distinct sedimentation modes and presented a phase diagram showing transitions between these modes as the blockage ratio varies. [5] numerically investigated the behavior of general shaped particles (circular, square, and elliptical) in a concentric annular duct with an internal obstacle in the fluid domain. Their study focused on the influence of particle shape, size, initial position and Reynolds number on particle trajectories, revealing critical conditions under which particles migrate

towards the inner or outer boundary. [6] numerically investigated the sedimentation behavior of circular particles forming chain-like configurations in a vertical fluid channel using the fictitious boundary method within an Eulerian framework. They analyzed various initial particle arrangements and orientations to study DKT effects. They also compared the results obtained for trajectory and settling dynamics of the particles.

[7] utilized fully resolved direct numerical simulations of thermal convective suspensions of elliptic particles using a multigrid Finite Element Fictitious Boundary Method (FEM-FBM). They used a modified collision model for handling the interactions between circular and elliptic particles. The method was applied to investigate the effects of heat exchange, Grashof number and particle-particle interactions in large-scale suspensions with high efficiency of the model.[8] performed a computational study on the settling behavior of twin circular particles in a fluid using the fictitious boundary method (FBM) with the finite element approach. Their study focuses on the variation of Reynolds number and the particle initial horizontal spacing between pair of particles. They investigated the dynamics of particles through terminal velocity and at each configuration of Reynolds number and distinct particle-gap. [9] discussed the behavior of elliptical and rectangular particles falling in a vertical channel and compared the results obtained for the shapes of ellipse and rectangle. [10] conducted numerical simulations involving pentagon- and square-shaped particles, while [11] extended the investigation to more general shapes, including square and triangular particles .

Many collision models have been presented to handle the collision between two or more moving particles. Some of them are lubrication force models [12], repulsive force models [13, 14], models based on conservation of linear momentum and kinetic energy [15], stochastic collision models [16] and so on. In the present study, we utilize the repulsive force model developed by Glowinski *et al.* [17], which effectively prevents particle collisions and handles overlapping issues arising from numerical point of view. In the movement of particles, when a particle enters the wake of a neighboring particle, it tends to accelerate toward the leading particle a phenomenon influenced by particle shape, size and inter-particle spacing. The space-time finite element method is employed to obtain solutions and analyze numerical results. Furthermore, when two solid particles approach each other during settlement, lubrication forces become significant and help to model the collision process.

1.1 Novelty of work

The present article examines the computational analysis of non-circular shaped particles by using the fictitious boundary method combined with an Eulerian approach. The numerical investigation of the movement of these non-circular shaped particles has been conducted for different Reynolds number (Re), which are Re=100, 200, 300 and 1000. The analysis predicts the results for three different non-circular shaped particles which include triangle, square and pentagon for the said Reynolds numbers. The numerical results, such as minimum/maximum distance between falling particles at different time intervals and the terminal velocity obtained by each particle at each Reynolds number, have been presented for the analysis. Furthermore, the results have been displayed for snapshots, velocity profiles and trajectory mapping of twin particles. We noted the horizontal and vertical components of velocities of adjacent settling particles under the effect of gravity. Moreover, it is investigated that how particle shape significantly affects during sedimentation and their velocities. Through the numerical

computations it is analyzed the relationship between peak horizontal velocity and Reynolds numbers and also investigated the impact of the shape of the particle on particle dynamics.

2. MATHEMATICAL MODELLING

Consider the fluid flow containing n solid particles, the mass of i^{th} particle in the fluid is m_i, where (i = 1,2,3,· · ·,n), density of the particle is ρ, density of fluid is ρ_f and viscosity of fluid is v. The Ω is the total domain, which is given by,

$$\Omega = \Omega_f(t) \cup \Omega_i(t) \qquad \forall\, i \in (1,2,3,\cdots,n),$$

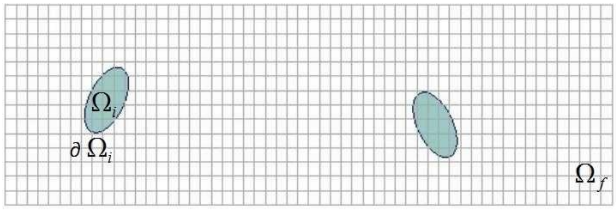

Figure 1: Domain containing fluid and particle

where, Ω_f, Ω_i denote the domain of fluid and domain occupied by i^{th} particle respectively and boundary for the i^{th} particle is represented by $\partial\Omega_i$ [18].

2.1 Incompressible Fluid

Navier-Stokes equations govern the motion of incompressible fluid in the computational domain [19, 20, 6]

$$\rho_f \left[\frac{\partial \mathbf{v}_f}{\partial t} + \mathbf{v}_f \cdot \nabla \mathbf{v}_f\right] - \nabla \cdot \alpha = \mathbf{0}, \;\; \nabla \cdot \mathbf{v}_f = 0 \;\; \forall\, t \in (0, t_{max}), \tag{1}$$

where α is the total stress tensor in the fluid defined as,

$\mathbf{v}_f + (\nabla \mathbf{v}_f)^{T}$. h (2)

The pressure is denoted by P, the fluid velocity is denoted by $\mathbf{v}_f$, μ_f is the viscosity coefficient and $\mathbf{I}$ is the identity tensor.

2.2 Motion of Particles

The freely moving solid particles in fluid acquire translational and rotational motion due to hydrodynamic forces, gravitational acceleration and the particle-particle and particle wall collision forces. If $\mathbf{U}_i$ and ω_i are the translational and angular velocities of the i^{th} particle respectively, then they satisfy,

$d\mathbf{U}i$

$$m_i \frac{}{dt} = (\triangle m_i)\,\mathbf{g} + \mathbf{F}_i + \mathbf{F}_i^c, \tag{3}$$

$$I_i \frac{d\omega_i}{dt} = \tau_i - \omega_i \times (I_i \omega_i), \tag{4}$$

$$\triangle m_i = m_i - m_f,$$

where, $\mathbf{F}_i$ and $\mathbf{F}^c{}_i$ are the drag/lift forces and collision forces acting on the particle respectively. But the mass of fluid m_f and mass of the particle m_i have same volume. The rotational effect is denoted by τ_i, I_i is the identity tensor the moment of inertia and $\mathbf{g}$ is the gravitational acceleration.

The position $\mathbf{x_i}$ of the center of mass of the i^{th} particle and its angle ϕ_i can be obtained after integrating the following equations [6, 21],

$$\frac{d\mathbf{x}_i}{dt} = \mathbf{U}_i, \qquad \frac{d\phi_i}{dt} = \omega_i. \tag{5}$$

We apply no-slip boundary conditions between the fluid and the particle, the velocity $\mathbf{v}_f$ is calculated as,

$$\mathbf{v}_f(\mathbf{x}) = \mathbf{U}_i + \omega_i \times (\mathbf{x} - \mathbf{x}_i). \tag{6}$$

2.3 The Drag and Lift Forces

The *drag/lift* force $\mathbf{F}_i$ and the rotational effect $\mathbf{T}_i$ acting on center of mass of the particle is given by [22],

$$\mathbf{F}_i = (-1) \int_{\partial\Omega_i} (\alpha \cdot \hat{n}) d\Gamma_i, \tag{7}$$

$$\mathbf{T}_i = (-1) \int_{\partial\Omega_i} (\mathbf{x} - \mathbf{x}_i) \times (\alpha \cdot \hat{n}) d\Gamma_i, \tag{8}$$

where $\hat{n}$ is the unit normal vector drawn outwards to the boundary of the particle.

2.4 Collision model for non-circular particles

We have chosen the collision models from different classes of collision models for analysis. Analysis of these collision models for circular particles is discussed by [18]. We have modified these collision model for non-circular shaped particles to handle the collision between particles while settling in the channel.

Initially the particles are considered circular (inscribed in a circle) and collision between such circular particles is detected.

If collision occurs between circumscribed circles, then again collision is detected for the original non-circular particles.

If collision occurs between non-circular particles then collision force is activated otherwise no force is required.

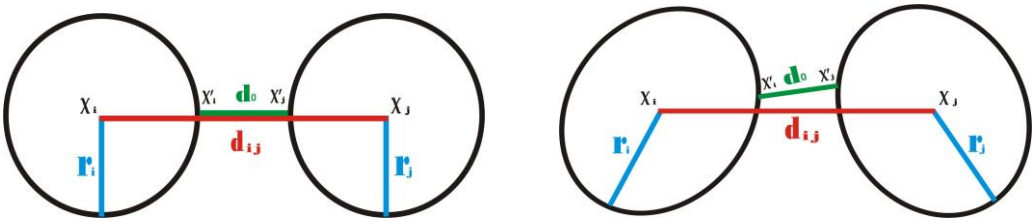

(a) Circular particle (b) Noncircular shaped particle

Figure 2: Schematic diagram for general shaped particles.

A lot of computational effort is required to calculate the minimum distance between non-circular particles as point to point distance from the surface of both particles need to be evaluated. Hence, particles are initially considered as circular which reduces a lot of computational cost. Similarly, collision forces acting on the circular particles are mostly normal to the surface but in case of non-circular particles, the rotational effect also comes into play [23]. Keeping these points, all the three collision models are presented in modified form given below:

2.4.1. Repulsive Force Model

It is a lubrication based model; it refers that the lubrication force between particles always exists. A collision model presented by [24] is modified to handle the particle-particle collision, which is given by

$$\mathbf{F}_{ij}^{c} = \begin{cases} 0 & , \quad d0 > \zeta, \\ \frac{1}{\beta_p}\left(\mathbf{x'}_i - \mathbf{x'}_j\right)\left(\zeta - d_0\right)^2 & , \quad 0 \le d_0 \le \zeta, \\ \frac{1}{\beta_p^c}\left(\mathbf{x'}_i - \mathbf{x'}_j\right)\left(-d_0\right) & , \quad d_0 \le 0, \end{cases} \tag{9}$$

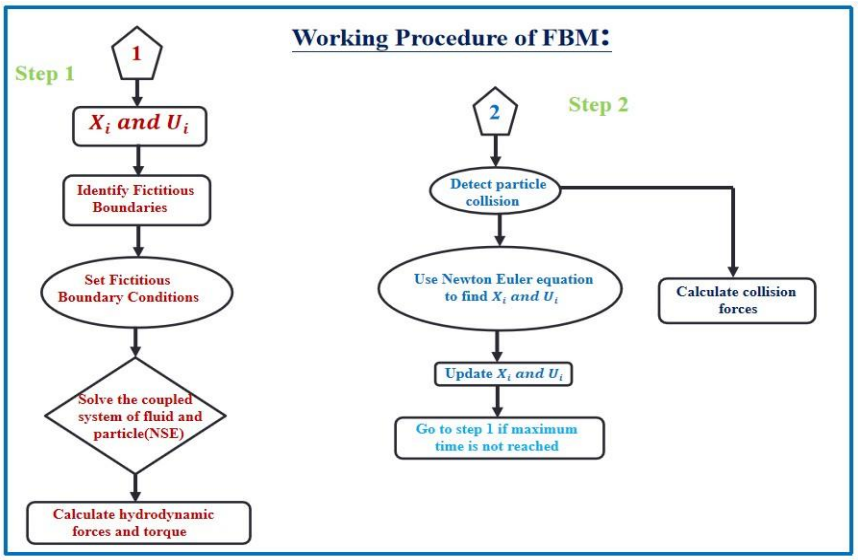

Figure 3: Working procedure of FBM

$$\mathbf{T}^i = (\mathbf{x}'_i - \mathbf{x}_i) \times \mathbf{F}^c_{ij}, \tag{10}$$

Here, $\mathbf{x}'_i$ and $\mathbf{x}'_j$ are the closest points on the surface of i^{th} and j^{th} particles, respectively. $d_0 = |\mathbf{x}'_i - \mathbf{x}'_j|$ is the surface-to-surface distance and $\mathbf{T}_i$ is the torque on the i^{th} particle.

The coordinates of the centres of the i^{th} particle are $\mathbf{x}_i$ and ζ is the minimum distance to activate the force of repulsion between particles. The values for the positive stiffness parameters β_p and β^c_p are chosen such as to avoid discontinuity or singularity [23].

3. FICTITIOUS BOUNDARY METHOD

In this method, the total domain contains both the fluid domain and the domain occupied by the particle. The multigrid finite element method (FEM) [19, 21] works in the background of the fictitious boundary method [23]. Since the domain of particle is changing its position in the whole domain at every moment that results to generate new boundary conditions. By including equation (6) as additional constraints to the Navier-Stokes equations, the Navier-Stokes equations take the form,

$$\begin{array}{l} \forall\, \mathbf{x} \in \Omega, \\ \\ \forall\, \mathbf{x} \in \bar{\Omega}_i, \end{array} \quad \begin{cases} \nabla \cdot \mathbf{v}_f = 0, \\ \rho_f \left(\frac{\partial \mathbf{v}_f}{\partial t} + \mathbf{v}_f \cdot \nabla \mathbf{v}_f \right) - \nabla \cdot \alpha = \mathbf{0} \\ \mathbf{v}_f(\mathbf{x}) = \mathbf{U}_i + \omega_i \times (\mathbf{x} - \mathbf{x}_i), \end{cases} \quad , \quad \forall\, \mathbf{x} \in \Omega_f, \tag{11}$$

$(i = 1,2,3,\cdots,n).$

4. NUMERICAL RESULTS

The numerical results have been obtained using a mesh refinement level 5 that guarantees mesh independence and there are 66304 number of elements on the mesh at this mesh refinement level. The computational mesh consists of 2 units in width and 8 units in height. The simulations have been performed for different particle shapes which include triangle, square and pentagon. The particle's density is 1.25 and of the fluid is kept 1.0, with the characteristic length of particle as 0.1. The twin particles fall freely in the vertical fluid domain through gravitational acceleration g = 980. Zero Dirichlet boundary conditions have been used at the boundary of the walls of the channel. The numerical results from simulations have been obtained with utilization of the CFD code FEATFLOW [25] at Reynolds number of Re = 100, 200, 300 and 1000. The numerical experiments are performed by considering three different shapes for particle with fixed initial horizontal gap between pair of particles i.e. 0.1, that indicates the first particle's position at (1.15,7.2) and second particle's position at (0.85,7.2).

The selected snapshots have been presented and have been shown in the figure 4, figure 5 and figure 6 for triangular, square and pentagonal shaped particles. Furthermore, we presented the results for trajectories of the particles settling in the channel as shown in figure 8. The x-and y-components of velocity profiles have been presented in the figure 7. The numerical results have been calculated in the tables 1 and 2 containing the data of minimum distance between pair of particles during the settlement of the twin particles. The figure 4 represents the results for each particle shape at time t = 0.0 (a-c) and t = 0.20 (d-f) having different Reynolds number. Similarly, for time t = 0.40 and t = 0.60 have been

displayed in the figure 5 and for time at $t = 0.80$ and $t = 1.00$ have been presented in the figure 6 for each configuration. From these figures we observe that square shaped particle reaches to bottom in the channel fastest followed by pentagonal and triangular shaped particles.

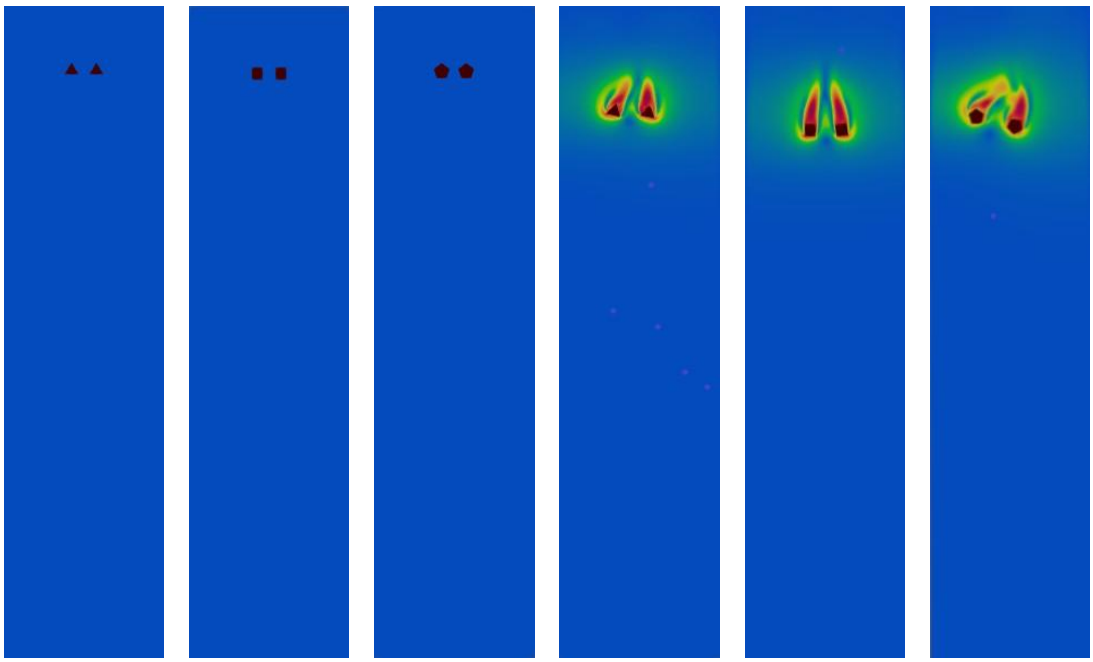

(a) Triangle (b) Square (c) Pentagon (d) Triangle (e) Square (f) Pentagon

Figure 4: Snapshots at time t=0.00 (a-c) and at t=0.20 (d-f) for particle pair of Triangle, Square and Pentagon at Re=100.

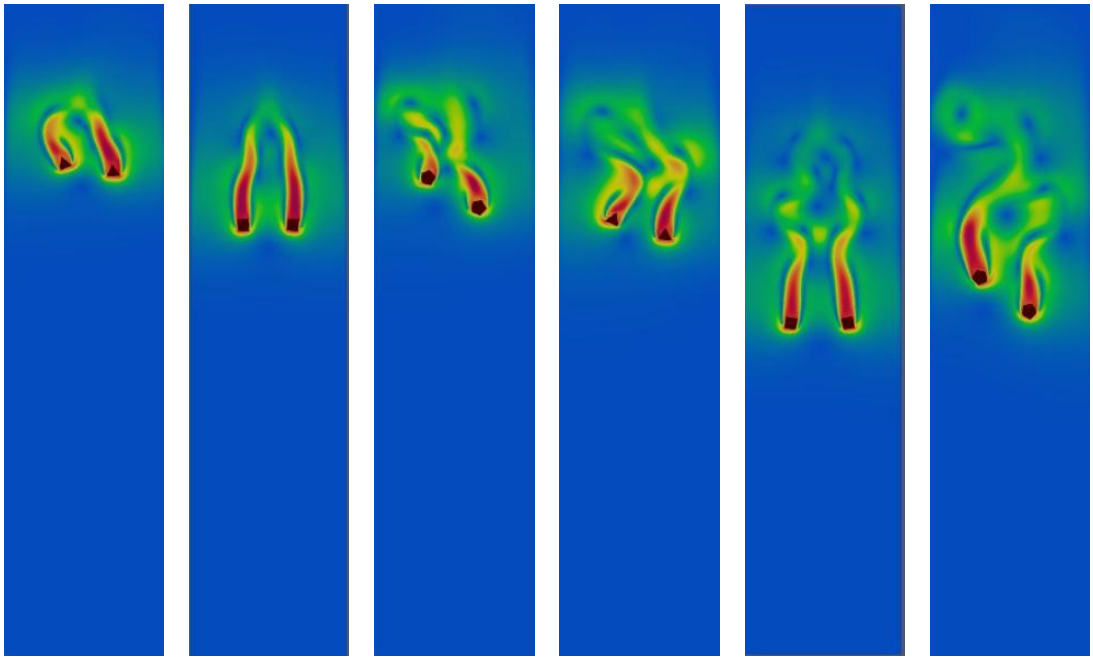

(a)Triangle (b) Square (c) Pentagon (d) Triangle (e) Square (f) Pentagon

Figure 5: Snapshots of twin particles at time t=0.60 (a-c) and at t=0.80 (d-f).

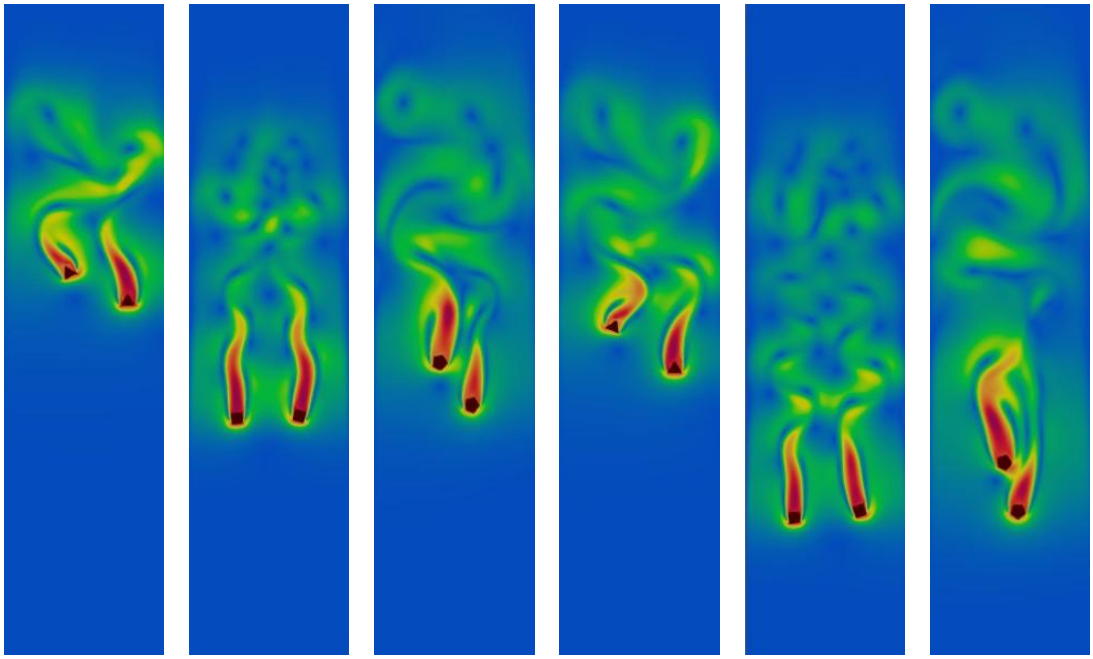

(a) Triangle (b) square (c) pentagon (d) Triangle (e) square (f) pentagon

Figure 6: Snapshots of twin particles at time t=0.80 (a-c) and at t=1.00.

The velocity profiles for the twin particles have been displayed in the figure7. In the graph, the first particle P_1 is denoted by (solid line) and the second particle P_2 is denoted by (dotted line) and the color scheme is reserved for triangle (red), square (blue) and pentagon (black). The numerical results for velocity and trajectory have been obtained at four Reynolds numbers $Re = 100, Re = 200, Re = 300$ and $Re = 1000$ for each particle shape. The figure 7 (a-d) shows the graphs for x-component (horizontal) of the falling particle and a pentagonal shaped particle predicts many fluctuations than other particle shapes. Similarly, a pentagonal particle experiences more oscillations for y-components of the velocity and almost all velocity profiles for V_y show an identical behavior for other particle shapes. The trajectory graphs of twin falling particles have been presented in the figure [**?**] and we can observe that the square shaped particle settles down fastest and reached to bottom earliest than other particles in the fluid channel. When we increase the Reynolds number the oscillation pattern for triangle become more prominent while pentagon and square get less oscillation pattern. Also, the square shaped particle experiences the least fluctuations even when Reynolds number jumps to 1000.

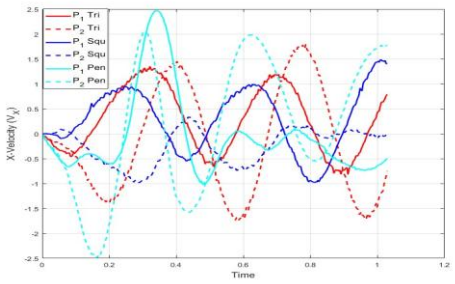

(a) V_x at Re=100

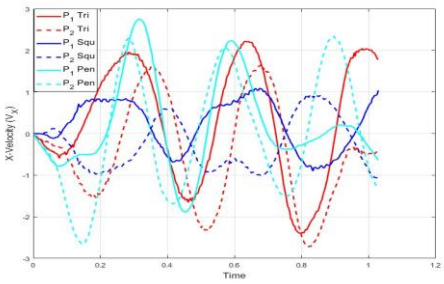

(b) V_x at Re=200

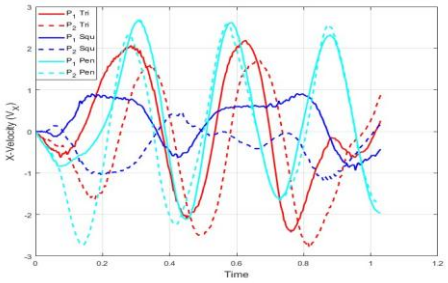

(c) V_x at Re=300

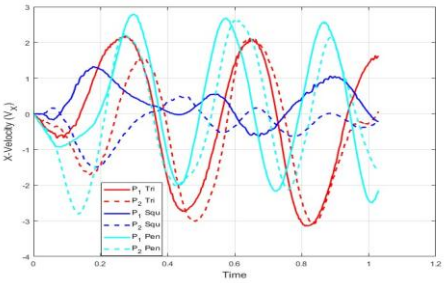

(d) V_x at Re=1000

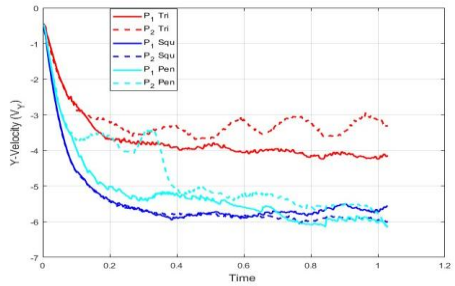

(e) V_y at Re=100

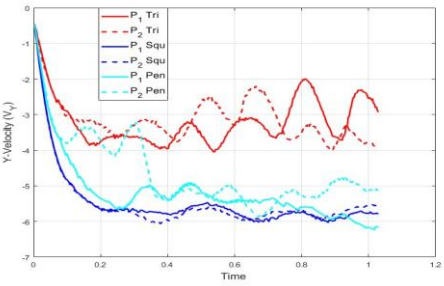

(f) V_y at Re=200

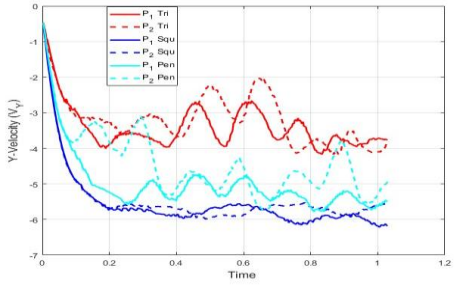

(g) V_y at Re=300

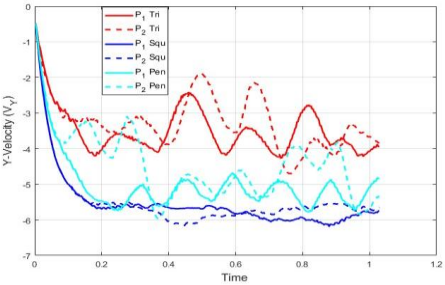

(h) V_y at Re=1000

Figure 7: Velocity profiles for different Reynolds number.

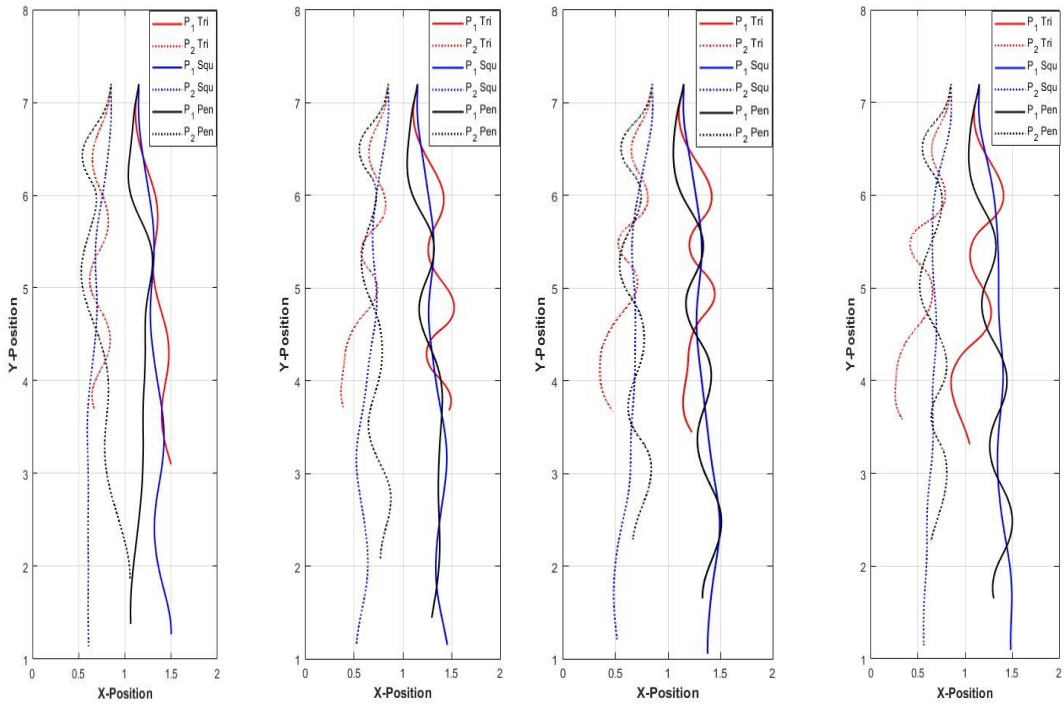

(a) Re=100 (b) Re=200 (c) Re=300 (d) Re=1000

Figure 8: Trajectories for Triangle, Square and Pentagon with different configurations.

Table 1: Minimum distance between twin particles indicating time and height.

No. of elements (at mesh refinement level-5)				**66304**
Re	**Shapes**	**Min Dist.**	**at Time**	**Height**
100	Triangle	0.11584	0.099	7.0253
	Square	0.14157	0.087	6.9661
	Pentagon	0.10717	0.057	7.0990
200	Triangle	0.11248	0.096	7.0158
	Square	0.14124	0.084	6.9600
	Pentagon	0.10712	0.054	7.0992
300	Triangle	0.11374	0.090	7.0265
	Square	0.14103	0.081	6.9662
	Pentagon	0.10704	0.051	7.1049
1000	Triangle	0.11292	0.087	7.0212
	Square	0.13521	0.078	6.9654
	Pentagon	0.10676	0.051	7.0962

The minimum distance between settling pair of particles and minimum velocities have been calculated and presented in the tables 1 and 2. The table 1 shows the minimum distances between twin particles

within the first zigzag loop for different Reynolds numbers with fixed initial horizontal distance between pair of particles. When the particle pair is settling down in the channel we notice that, at *Re* = 100, the minimum separation distance is observed 0.10717 for pentagon at time 0.057 with height of 7.0990 at that time. Whereas for triangle, the minimum separation distance is recorded to 0.11584 at time 0.099 and height 7.02530. For square, the minimum separation distance is noted that 0.14157 at time 0.087 and height 6.96610. Other cases for Reynolds number, 200, 300 and 1000, the results have been presented in this table 1. It can be observed that with different Reynolds number, overall the minimum distance has been achieved by pentagonal particle shape which is 0.10676 at time 0.051 when the particles were at a height of 7.0962. It is observed that the particles move apart from each other and then come close to each other while settling in the fluid domain, then they achieve the minimum spacing between twin particles. This process continues until the particles reach to the bottom of the channel and a wiggly trajectory of particles is formed.

The table 2 provides data for the velocity of x-component V_x (horizontal velocity) and y-component V_y (vertical velocity) of settling particles of different shapes (triangle, square and pentagon) under different Reynolds numbers. Analysis reveals that the particle shape has a crucial influence on settling velocities. The square shaped particle consistently demonstrates the lowest terminal velocities V_x across all Reynolds numbers. For example, at *Re* = 100, the V_x of the square is −0.9855, which is smaller than that of the pentagonal and triangular shaped particles under the same conditions. This phenomenon suggests that the square shaped particle is less influenced by hydrodynamic forces and enables the particle to achieve lower velocity. In contrast, the triangular shaped particle have a velocity of −1.7368 at height 4.7911 and at time = 0.585, which is

Table 2: Minimum x-and y-velocity of the particles at different *Re*

No. of elements (at mesh refinement level-5)						**66304**	
Re	**Shapes**	**Min V_X**	**at Time**	**Height**	**Min V_Y**	**at Time**	**Height**
100	Triangle	-1.7368	0.585	4.7911	-3.1803	0.198	4.8197
	Square	-0.9856	0.285	2.3574	-5.4364	0.198	2.5636
	Pentagon	-2.4859	0.165	4.4805	-3.7779	0.117	4.2221
200	Triangle	-2.7193	0.816	4.6673	-3.2905	0.198	4.7095
	Square	-1.0832	1.035	2.4597	-5.6692	0.198	2.3308
	Pentagon	-2.6576	0.144	4.5484	-3.8170	0.093	4.1830
300	Triangle	-2.7714	0.816	4.2334	-3.3445	0.198	4.6555
	Square	-1.1765	0.858	2.2407	-5.6801	0.192	2.3199
	Pentagon	-2.7270	0.144	4.6527	-3.8445	0.090	4.1555
1000	Triangle	-3.0810	0.840	4.2758	-3.3204	0.195	4.6796
	Square	-1.4978	0.189	2.4112	-5.6082	0.180	2.3918
	Pentagon	-2.8152	0.135	4.6257	-3.9666	0.198	4.0334

lower than that of the pentagonal shaped particle. Whereas in case of V_y, at *Re* = 100, the y-velocity of the triangle is −3.1803 at height of 4.8197 and at time 0.198 which is smaller than that of the pentagonal

and square shaped particles under the same conditions. Similarly, the results for Re = 200, Re = 300 and Re = 1000 can be observed from the table 2. The data also highlights the impact of Reynolds number (Re) on settling velocities. With increasing Reynolds number, the x-component of velocity increases for all particle shapes in general. This trend is observed across all the particle shapes, indicating that as the Reynolds number rises, the particles experience greater inertial forces. This pattern reflects the transition from laminar to turbulent flow with increasing Reynolds number, where turbulent flow causes higher drag on the particle.

5. CONCLUSION

In this article, the numerical experiments have been performed using a fictitious boundary method and the finite element method. The results have been presented for three non-circular particle shapes, namely: an ellipse, a rectangle and a square, settling in the fluid domain at different Reynolds number. A fine mesh at mesh-refinement level 5 has been employed, which guarantees mesh independence, and it has 66304 number of elements in the computational grid. The major objective of the work is to investigate the impact of Reynolds number on particle shape. The outcomes of the research work may significantly enhance the understanding of behavior of twin particles. Furthermore, the numerical approach utilizing the finite element method can increase the efficiency of the systems, especially in case of non-circular particle shapes. The results in Reynolds number perspective have been discussed earlier for circular shaped particles, the undergoing study comprises the results for non-circular shaped particles. We have computed the numerical results at four different Reynolds numbers Re = 100,200, 300 and 1000 having fixed starting positions of the twin particles. The particles' interaction is analyzed by presenting the snapshots, graphs for velocity profiles and trajectories of pair particles settling in the fluid domain. The tables contain the data for minimum distance between twin particles during fall indicating time and height at which the minimum distance is achieved. Similarly, minimum x- and y-velocity indicating the time and height of the particle is presented for each particle shape and distinct Reynolds number. The results presented in trajectory graphs and in the tabular form, we can observe that the square shaped particle settles down fastest and reached to bottom earliest than other particles. In other words, the terminal velocity of square increases because it experiences less hydrodynamic force and DKT process. On the other hand, when we come across by increasing Reynolds number, the flow changes from Laminar to turbulent and predicts many fluctuations than the lower Reynolds numbers. The triangular shaped particle has greatest influence of hydrodynamic forces than other particle shapes (square and pentagon) and we also conclude that the horizontal velocity increases gradually with increasing Reynolds number (Re).

CONFLICT OF INTEREST

On behalf of all authors, the corresponding author confirms that there is no conflict of interest associated with this work.

REFERENCES

[1] Zhaokai Hou, Enyuan Jiang, Ye Chen, Huaishan Wang, Jinyu Feng, and Xutao Tao. A novel prediction model of the drag coefficient of irregular particles in power-law fluids. *Processes*, 11(11):3213, 2023.

[2] K Usman, K Walayat, R Mahmood, and N Kousar. Analysis of solid particles falling down and interacting in a channel with sedimentation using fictitious boundary method. *AIP Advances*, 8(6), 2018.

[3] M Shahid, K Usman, and Afraz Hussain Majeed. Computational investigation of drag forces on bluff bodies induced by interacting non-circular particles in a vertical channel using the fictitious boundary method. *Physics of Fluids*, 37(4), 2025.

[4] Zhenhua Xia, Kevin W Connington, Saikiran Rapaka, Pengtao Yue, James J Feng, and Shiyi Chen. Flow patterns in the sedimentation of an elliptical particle. *Journal of Fluid Mechanics*, 625:249–272, 2009.

[5] S Jabeen, K Usman, and M Shahid. Numerical study of general shape particles in a concentric annular duct having inner obstacle. *Computational Particle Mechanics*, 9(3):485–497, 2022.

[6] Saqia Jabeen, Kamran Usman, and Khuram Walayat. Numerical investigations for a chain of particles settling in a channel. *Computational Particle Mechanics*, 7(4):615–627, 2020.

[7] Khuram Walayat, Zhilang Zhang, Kamran Usman, Jianzhong Chang, and Moubin Liu. Fully resolved simulations of thermal convective suspensions of elliptic particles using a multigrid fictitious boundary method. *International Journal of Heat and Mass Transfer*, 139:802–821, 2019.

[8] Imran Abbas and Kamran Usman. Computational study of twin circular particles settling in fluid using a fictitious boundary approach. *Int. J. Emerg. Multidisciplin. Math*, 2:1–12, 2023.

[9] Satoshi Yokojima, Ryu Takashima, Hideyoshi Asada, and Takashi Miyahara. Impacts of particle shape on sedimentation of particles. *European Journal of Mechanics-B/Fluids*, 89:323–331, 2021.

[10] Xiaowu Fu, Zhaohui Yao, and Xiwen Zhang. Numerical simulation of polygonal particles moving in incompressible viscous fluids. *Particuology*, 31:140–151, 2017.

[11] Anthony Wachs. A dem-dlm/fd method for direct numerical simulation of particulate flows: Sedimentation of polygonal isometric particles in a newtonian fluid with collisions. *Computers & Fluids*, 38(8):1608–1628, 2009.

[12] Bertrand Maury. A many-body lubrication model. *Comptes Rendus de l'Acad´emie des Sciences-Series I-Mathematics*, 325(9):1053–1058, 1997.

[13] Decheng Wan and Stefan Turek. Fictitious boundary and moving mesh methods for the numerical simulation of rigid particulate flows. *Journal of Computational Physics*, 222(1):28–56, 2007.

[14] N Zhang and ZC Zheng. A collision model for a large number of particles with significantly different sizes. *Journal of Physics D: Applied Physics*, 40(8):2603, 2007.

[15] Neelesh A Patankar, Pushpendra Singh, Daniel D Joseph, Roland Glowinski, and TW Pan. A new formulation of the distributed lagrange multiplier/fictitious domain method for particulate flows. *International Journal of Multiphase Flow*, 26(9):1509– 1524, 2000.

[16] Martin Sommerfeld. Validation of a stochastic lagrangian modelling approach for inter-particle collisions in homogeneous isotropic turbulence. *International Journal of Multiphase Flow*, 27(10):1829–1858, 2001.

[17] Roland Glowinski. Finite element methods for incompressible viscous flow. *Handbook of numerical analysis*, 9:3–1176, 2003.

[18] Kamran Usman. *Numerical Analysis of Collision Models in 2D Particulate Flow*. PhD thesis, Technische Universitaet Dortmund, Fakultaet fuer Mathematik, 2013.

[19] V. John. Higher order finite element methods and multigrid solvers in a benchmark problem for the 3d navier-stokes equations. *Int. J. for Numerical Methods in Fluids*, 40:775–798, 2002.

[20] John F. Wendt, editor. *Computational Fluid Dynamics*. Springer Berlin Heidelberg, 2009.

[21] Decheng Wan, Stefan Turek, and Liudmila S. Rivkind. An efficient multigrid fem solution technique for incompressible flow with moving rigid bodies. In Miloslav Feistauer, Vit Dolejsi, Petr Knobloch, and Karel Najzar, editors, *Numerical Mathematics and Advanced Applications*, pages 844–853. Springer Berlin Heidelberg, 2004.

[22] S. Kim S. and S. J. Karrila. *Microhydrodynamics: Principles and Selected Applications*. Butterworth-Heinemann, Boston, second edition, 1991.

[23] Muhammad Shahid and Kamran Usman. Kinetics of suspended particles with different shapes interacting in a fluid channel. *Computational Particle Mechanics*, 11:1–13, 11 2023.

[24] N.A. Patankar, P. Singh, D.D. Joseph, R. Glowinski, and T.W. Pan. A new formulation of the distributed lagrange multiplier/fictitious domain method for particulate flows. *Int. J. Multiphase Flow*, 26:1509–1524, 2000.

[25] S. Turek. Featflow. finite element software for the incompressible navier-stokes equations: User manual, release 1.1. Technical report, 1998.